5-2023

Using DNA as Scaffolding for the Study of FRET Enhancement by Surface Plasmons on Gold Nanogratings

Evan Thomas Engelhaupt
Trinity University, evanengelhaupt@gmail.com

Using DNA as Scaffolding for the Study of FRET Enhancement by Surface Plasmons on Gold Nanogratings

Evan T. Engelhaupt

A DEPARTMENT HONORS THESIS SUBMITTED TO THE
DEPARTMENT OF PHYSICS AND ASTRONOMY AT TRINITY UNIVERSITY
IN PARTIAL FULFILLMENT OF THE REQUIREMENTS FOR GRADUATION WITH
DEPARTMENTAL HONORS

DATE April 14, 2023

THESIS ADVISOR

DEPARTMENT CHAIR

Jennifer Henderson, AVPAA

Student Agreement

I grant Trinity University ("Institution"), my academic department ("Department"), and the Texas Digital Library ("TDL") the non-exclusive rights to copy, display, perform, distribute and publish the content I submit to this repository (hereafter called "Work") and to make the Work available in any format in perpetuity as part of a TDL, digital preservation program, Institution or Department repository communication or distribution effort.

I understand that once the Work is submitted, a bibliographic citation to the Work can remain visible in perpetuity, even if the Work is updated or removed.

I understand that the Work's copyright owner(s) will continue to own copyright outside these non-exclusive granted rights.

I warrant that:

1) I am the copyright owner of the Work, or
2) I am one of the copyright owners and have permission from the other owners to submit the Work, or
3) My Institution or Department is the copyright owner and I have permission to submit the Work, or
4) Another party is the copyright owner and I have permission to submit the Work.

Based on this, I further warrant to my knowledge:

1) The Work does not infringe any copyright, patent, or trade secrets of any third party,
2) The Work does not contain any libelous matter, nor invade the privacy of any person or third party, and
3) That no right in the Work has been sold, mortgaged, or otherwise disposed of, and is free from all claims.

I agree to hold TDL, DPN, Institution, Department, and their agents harmless for any liability arising from any breach of the above warranties or any claim of intellectual property infringement arising from the exercise of these non-exclusive granted rights."

I choose the following option for sharing my thesis (required):

[✓] Open Access (full-text discoverable via search engines)
[ ] Restricted to campus viewing only (allow access only on the Trinity University campus via digitalcommons.trinity.edu)

I choose to append the following Creative Commons license (optional):

Acknowledgements

I would like to thank my research advisor and chair of the Trinity University Department of Physics and Astronomy, Dr. Jennifer Steele, for being an integral part in guiding my work and this thesis for the last three years. Additionally Andra Key, my research partner, aided me greatly in the fabrication, AFM characterization, and transmission analysis of the gold nanogratings. Dr. Orrin Shindell of the Trinity University Department of Physics and Astronomy provided the Epifluorescence microscope that much of our data was taken on. Dr. Hoa Nguyen from the Trinity University Department of Mathematics also assisted in optimizing and troubleshooting my MATLAB code. My thanks go out to all of them. I would also like to thank the entire physics department for assisting and editing and revising this thesis in its final stages.

This work is largely interdisciplinary and would not have been possible without the assistance and the advising of the Trinity University Chemistry Department, notably Dr. Corina Maeder, Dr. Christina Cooley, and Dr. Adam Urbach. Dr. Maeder was instrumental in advising our design of the annealing procedure and lent her expertise on how to best store and handle DNA strands. Dr. Christina Cooley assisted in determining the dipole orientation of our Cy3 molecule, and Dr. Urbach assisted in troubleshooting our procedure for DNA attachment to glass.

Lastly, this work would not be financially possible without the help of the National Science Foundation, under Grant no. 2004681, who provided the grant for this research to be carried out.

Table of Contents

Table of Figures

I. Introduction

Fluorescent molecules, or fluorophores, are molecules commonly used as tags in biosensing applications. Fluorophores absorb light at specific wavelengths, elevating the energy of an electron in the molecule to an excited state. Energy is then emitted as a photon from the fluorescent molecule, bringing the electron back to its ground state. The emitted photon typically carries less energy and thus the light emitted has a longer wavelength. As an example of this phenomenon, Cyanine-3, or Cy3, is a fluorescent molecule that has peak absorption of light at around 555nm (green light) and an emission peak at around 569nm, thus appearing an orange-pink color in solution.

Förster Resonance Energy Transfer is a process can occur between two fluorescent molecules where one acts as a donor and the other acts as an acceptor. If the emission spectra of the donor overlaps with the absorption spectra of the acceptor (illustrated in Figure 1), then energy transfer can occur between the two molecules. Figure 2 depicts this process using a Jablonski diagram.

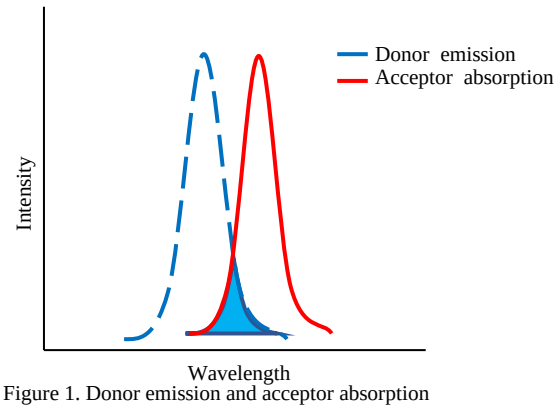

Figure 1. Donor emission and acceptor absorption spectral overlap

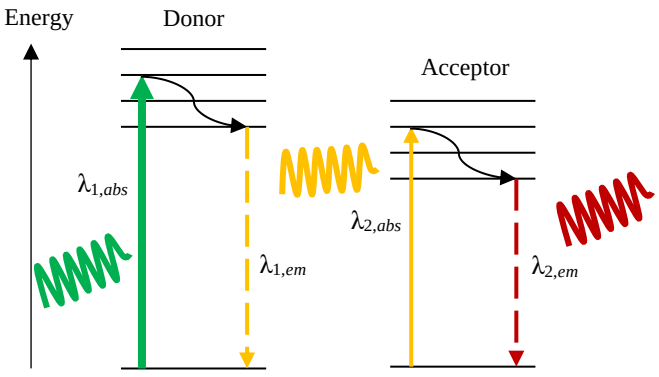

Figure 2. FRET between a donor and acceptor molecule depicted in an energy diagram.

Figure 2 shows green light is absorbed by the donor molecule, raising an electron to an excited state. The spectral overlap exists between donor and acceptor, as presented in Figure 1, the

energy released from the electron decay back to the ground state is transferred to an electron in the acceptor. Such donors and acceptors are termed FRET pairs. The acceptor electron decays, releasing a photon with wavelength corresponding to red light. FRET is heavily dependent on distance, scaling as $1/r^6$, and small changes in the distance between the donor and acceptor would thus have profound effects on the probability of FRET occurring. The distance at which the FRET process is 50% efficient is called the Förster radius and is often on the nanometer scale. FRET is useful in biological studies as a measuring device. For instance, an enzyme can be tagged with a donor and a substrate the acceptor. When the enzyme and substrate bind to each other, FRET will occur between the two molecules, thereby signaling that attachment has occurred. The information on FRET is drawn from Lakowicz, 2006.

This work seeks to enhance the FRET efficiency via fine tuning the distance of the donor and acceptor molecules relative to metal surfaces which exhibit surface plasmons. Surface plasmons are longitudinal waves of conduction electrons that travel along the surface of a metal. Metal surfaces exhibiting surface plasmons can enhance the fluorescence of donor and acceptor molecules via metal enhanced fluorescence (MEF). Surface plasmons and MEF are discussed in more detail in Section II. Regarding FRET, surface plasmons can enhance FRET efficiency by offering an alternate decay channel (Figure 3). Fermi's Golden Rule states that the increase in the number of decay channels will shorten the lifetime of the excited state of the electron in both the donor and the acceptor (Steele, et al., 2017).

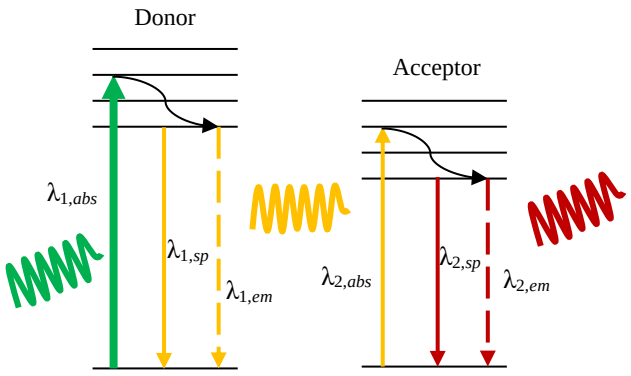

Figure 3. Alternate emission pathway offered by a surface plasmon to enhance FRET by shortening the lifetime of the excited state.

For this work, gold nanogratings were used. Surface plasmons on a nanograting are travelling waves that follow a dispersion relationship, allowing for a broad range of surface plasmon wavelengths to be accessed (Rather, 1998). The fabrication of nanogratings and their characterization are described in Section III.

To fine tune the distance of the donor and acceptor molecules relative to the metal surface, DNA can serve as scaffolding (see Section IV). Strands of DNA were ordered containing fluorescent molecules various distances along the backbone. These strands were then chemically attached upright to the gold surface, thereby positioning the fluorophore above the gold at a known distance for FRET analysis. Section IV details the attachment methods used and optimization techniques to get high densities of DNA containing fluorophore attachments onto the gold substrate. Detailed in Section V are failures and successes of various fluorophore positions along the DNA backbone and recommendations going forward.

II. Surface Plasmons and Metal Enhanced Fluorescence

i. Surface plasmons on gold nanogratings

On smooth metal films, surface plasmons exhibit a dispersion relationship given by

$$k_{sp} = \frac{\omega}{c}\left(\frac{\epsilon_1 \epsilon_2}{\epsilon_1 + \epsilon_2}\right)^{1/2} \qquad (1)$$

where $k_{sp} = \frac{2\pi}{\lambda_{sp}}$ is the wavevector along the metal (λ_{sp} is the wavelength of the surface plasmon), ω is the frequency of the incident light, c is the speed of light, ϵ_1 is the frequency dependent dielectric function of the metal, and ϵ_2 is the frequency dependent dielectric function of the medium surrounding the metal (Raether, 1998). Typically for smooth films surrounded by air, this dispersion relation falls outside the light cone. On metal gratings, however, the periodic structure allows for direct excitation through momentum matching. Specifically, the grating allows for an integer number of reciprocal lattice vectors to be added to the wavevector of light parallel to the surface. Figure 4 depicts the resulting surface plasmon wavelength, λ_{sp}, for light incident at some angle, θ, relative to the surface normal. Since the surface plasmon along the surface is only excited by the component of light parallel to the surface, we can express the surface light wavevector as

$$k_{surf} = k_0 sin\theta + mG \qquad (2)$$

where k_{surf} is the component of the vector along the surface, k_0 is the wavevector of incident light, m is the diffraction order ($m = 1$ in most of this work), and $G = \frac{2\pi}{d}$ is the reciprocal lattice vector (d is the period of the grating). When k_{surf} and k_{sp} are equal, a surface plasmon is excited on the grating surface (Raether, 1998).

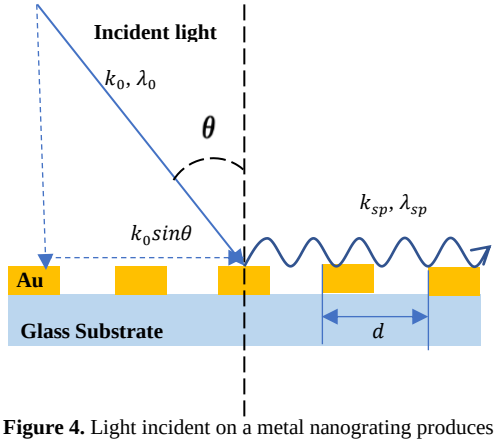

Figure 4. Light incident on a metal nanograting produces a travelling surface plasmon wave with a specific wavelength.

ii. Metal Enhanced Fluorescence

It has been shown experimentally that surface plasmons on a metal nanoparticle or a metal surface can modify a fluorophore's emission when in proximity to the molecule. These modifications rely on spectral overlap between the surface plasmon and the emission or absorption spectra of the fluorophore. In cases where the surface plasmon wavelength overlaps with the absorption spectra of the fluorophore, the excitation of the fluorophore's electron is enhanced (Hure et al., 2016). When the surface plasmon wavelength overlaps with the emission spectra of the fluorophore, there is an increase in the local density of optical states (LDOS). LDOS refers to the number of electromagnetic modes that can be occupied by a photon. An increase in LDOS thereby increases the number of decay channels through which the excited electron can return to the ground state; the electron can either emit a photon, as expected without a surface plasmon, or excite the surface plasmon. Fermi's Golden Rule states that an increase in decay channels shortens the lifetime of the excited state of the fluorophore, thereby increasing the emission rate (Novotny and Hecht, 2021). Both mechanisms have been verified experimentally (Steele et al., 2010; Hure et al., 2016, Steele et al. 2017).

Metal gratings in particular hold several advantages in the application of MEF over other metal surfaces such as nanoparticles. Primarily, the increased emission rate (shortening of the lifetime of the excited state) has been shown to be the dominant mechanism. The enhanced excitation has a smaller but measurable effect on overall MEF (Steele et al., 2010). Additionally, gratings make it possible for the fluorophores to couple to multiple surface plasmon modes on both the air and substrate (glass in this work) side of the grating (Steele et al., 2010). This prediction was verified experimentally after enhanced fluorescence associated with surface plasmon modes was observed on both the air side and substrate side of the grating. Compared to other metal structures, such as corrugated systems, which have weak coupling on the side of the substrate, gratings offer a notable improvement. Metal gratings also exhibit equal coupling to higher surface plasmon modes as opposed to corrugated surfaces which showed weaker enhancement from the higher diffraction modes (Steele et al., 2010). Because these higher surface plasmon mode wavelengths are fractions of the grating period, metal gratings with periods of microns and above can enhance fluorescence in the visible range, making fabrication of the grating easier.

iii. MEF applied to FRET

MEF can enhance the energy transfer rate of FRET through the enhancement of the excitation and the increase in LDOS. The Förster radius defines the distance at which FRET is 50% likely to occur in a FRET pair. Often, this radius is between 1nm and 10nm. By increasing the transfer rate, the Förster radius increases. Utilizing the dispersion relationship of surface plasmons on a gold nanograting, earlier work from this lab investigated the effect of a LDOS increase at three points throughout the FRET process: donor emission wavelengths, acceptor

emission wavelengths, and where the ranges overlap. By selecting surface plasmon wavelengths on a grating that corresponded to each of these categories, FRET efficiency was calculated as a function of surface plasmon wavelength. It was observed that the largest increase in FRET efficiency occurred when surface plasmon wavelengths overlapped with the acceptor emission spectrum, thereby increasing the LDOS at that emission. As the LDOS increased, the acceptor molecules were allowed to decay to the ground state at a faster rate, making them more available for FRET transfer. This effect was observed less so when the surface plasmon wavelengths overlapped with the donor emission spectrum. An increase in the LDOS at the donor emission opens a competing channel against FRET, allowing donor electrons to decay to ground by exciting a surface plasmon rather than emitting a photon for the acceptor to reabsorb (Steele et al., 2017).

III. Grating Fabrication and Characterization

i. Fabrication

Gold nanogratings with a height and a period of 50nm and 555nm, respectively, were fabricated from silicon master gratings using a 184 Polydimethylsiloxane (PDMS) template stripping process. The silicon nanogratings were purchased from LightSmyth Technologies and had a period of 555nm, a height of 120nm, and a wire width of 250nm. Figure 5 illustrates the process of template stripping, which allows for inexpensive copies of the silicon grating to be produced. The silicon grating was first coated with about a 0.5cm tall layer of PDMS solution (Figure 5a), which was a mixture of silicone elastomer base and a 10% by weight amount of silicone elastomer curing agent. The PDMS was then cured in an oven at 80℃ for one hour. After curing, the silicon master grating can be peeled off and set aside for repeated usage while the imprint of the grating remains on the PDMS sample.

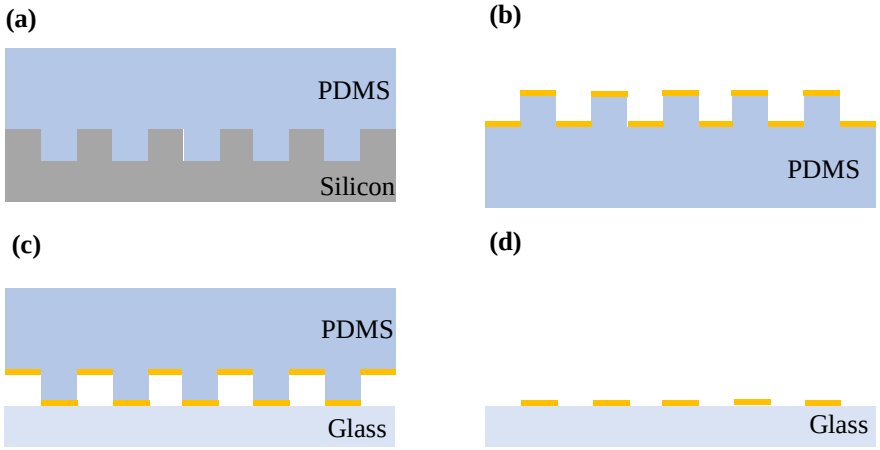

Figure 5. PDMS Template stripping process. **(a)** PDMS fills the gaps in the silicon nanograting. **(b)** After curing, the silicon nanograting is peeled off and the PDMS copy is coated with gold. **(c)** The coated PDMS sample is adhered onto glass and left to sit overnight. **(d)** the PDMS is peeled off leaving a gold nanograting on the glass.

Prior to adhering the PDMS to the glass slide, the glass was cleaned in acetone for 20 minutes, washed with ethanol followed by an 18.2 MiliQ water rinse, and immediately dried under nitrogen gas. 50nm of gold film was deposited on the PDMS via sputter coater (Figure 5b). a thin layer of 2-part, 5-minute epoxy was applied to the glass followed by the immediate

application of the PDMS sample gold side down (Figure 5c). PDMS-glass samples were left to sit overnight before the PDMS was carefully peeled off, leaving behind a gold nanograting on the glass slide (Figure 5d).

ii. Characterization

We verify the quality of the gold nanograting sample using atomic force microscopy (AFM). Operating in tapping mode, the AFM oscillates the cantilever near resonance frequency and rasters the cantilever across the sample, intermittently coming very close to the nanograting surface. The forces between the tip and the surface modify the cantilever's amplitude and frequency. To compensate for these changes, the AFM raises and lowers the cantilever to maintain the initial amplitude and frequency. The changes in position of the cantilever are then used to reconstruct a topology, as seen in the micrograph displayed in Figure 6. Figure 6a displays a top-down view of the gold nanowires, and Figure 6b depicts the cross section of the same sample with height and width measurements for the nanowires. With this topographic scan,

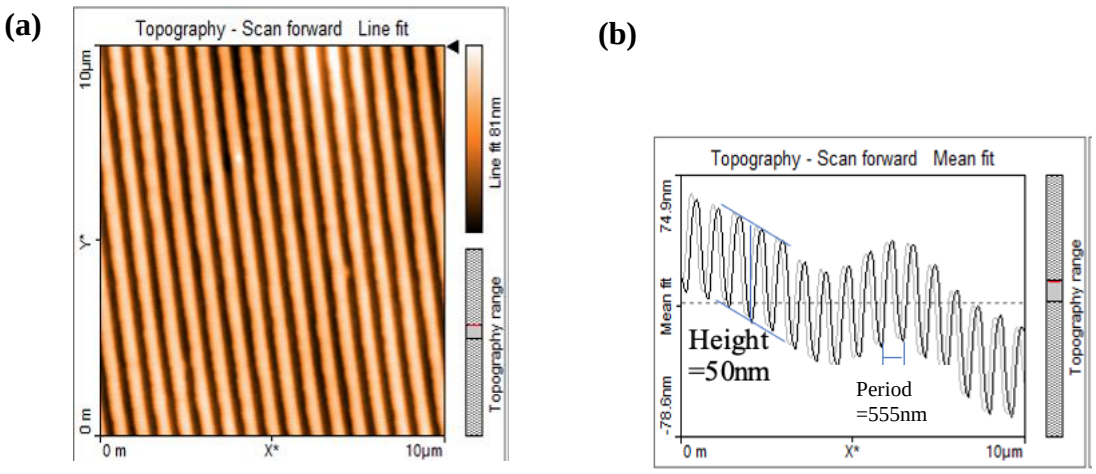

Figure 6. AFM Data for a gold nanograting sample. (a) depicts the top-down topographic scan. (b) shows the cross section of the same sample, from which we obtain values for height and period. Figures generated by Andra Key, Trinity University.

the height and period of the nanowires can be measured. For the sample given in Figure 6, the height and period come out to the expected 50nm and 500nm, respectively.

The second step of the characterization process was transmission. With white light transmission, one can measure the surface plasmon dispersion relationship. Light from a 100W tungsten halogen bulb was polarized, collimated, and shown onto the sample, which sat in a rotating sample holder. The sample was rotated in one-degree increments such that light was incident from 0° to 50° from the surface normal. As we turn the sample, thus adjusting the incident angle, Equation 2 shows that the surface plasmons are excited at a corresponding wavelength for every angle, allowing us to plot a dispersion relationship. After passing through the sample, the light beam was collected into a fiberoptic located directly behind the sample and connected to a linear silicon CCD array detector purchased from Ocean Optics (USB4000). Figure 7 shows dispersion relationships measured from this process for two different samples.

(a) **(b)**

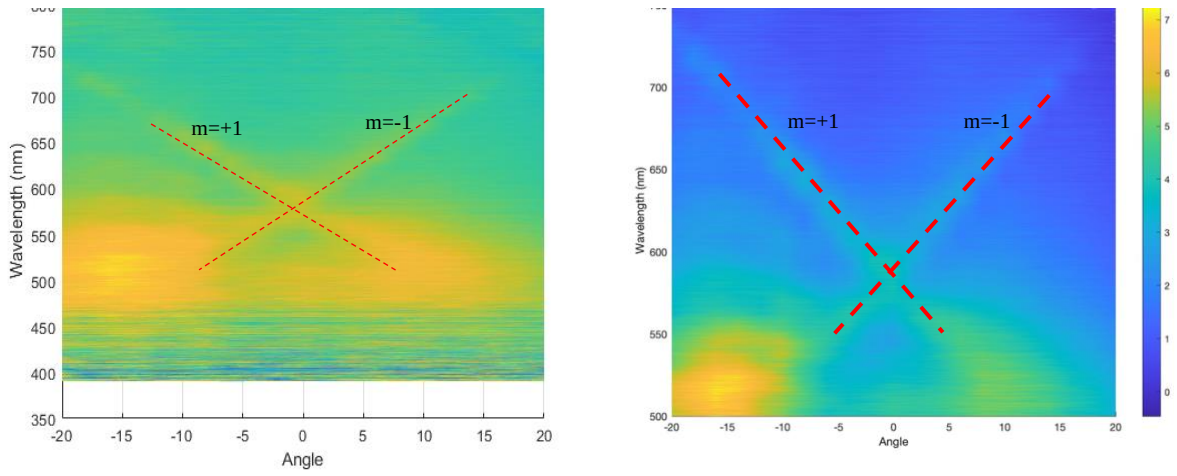

Figure 7. Transmission data for two gold nanograting samples. **(a)** is the same sample presented in Figure 6. **(b)** is a different sample with clearer surface plasmon peaks. Data taken by Andra Key, Trinity University.

The dispersion relationship shows two plasmon modes as peaks. Dashed lines have been added to guide the eye. When the incident angle is 0, Equation 2 indicates that the surface plasmon wavelength should just be the periodicity of the grating for first order (m=1) plasmons. For a 555nm grating period, we expect of wavelength of 555nm, which is observed in both graphs. The lines on both Figure 7a and Figure 7b indicates the presence of a first-order, air side plasmon with m=+1 and m=-1. One surface plasmon is red moving and another is blue moving. If one were to shine a green laser (532nm) on both samples depicted in Figure 7, the air side surface plasmon would be expected to excite at angle in the range of -5° or 5°. When running fluorescence experiments (see Section V), we chose 40° as our starting angle so that the laser does not excite the surface plasmon. Thus, we ensure that any plasmon excitation comes from fluorescence. This use of the dispersion relationship guided the selection of angle ranges during later fluorescence measurements.

IV. Using DNA as Scaffolding

In previous experiments by this lab, donor and acceptor molecules were distributed isotopically in solution and then spin coated onto the active side of the gold nanograting. Under this method, the distance between donor and acceptor was a calculated average based on concentrations and the precise distance to the grating surface was unknown. The precise positioning of donor and acceptor molecules relative to the surface of a gold nanograting is instrumental in understanding the effects of surface plasmons on the enhancement of FRET. We introduce DNA as scaffolding to hold donor and acceptor molecules a precise distance away from the gold nanograting surface. The spatial parameters of DNA are well known, and oligonucleotide strands can be ordered with fluorescent modifications practically anywhere along the backbone of the strand or on either 3' or 5' terminal end. Terminal attachments can also be modified to allow for bonding to our gold nanogratings. In this respect, DNA strands can theoretically bond to the gold surface on one end while the other end sticks straight up with a fluorescent molecule attached. The length of the DNA strand then defines the distance of the fluorescent molecule from the surface.

DNA strands were first attached to the gold surface with our donor of choice, Cyanine-3 (Cy-3), terminally attached to the other end. The acceptor molecule, Cyanine-5 (Cy-5), was left out until we verified attachment and fluorescence detection of the Cy-3 on the gold. Initial experiments used two 20 monomer, complimentary oligonucleotides that were ordered from Sigma-Aldrich and annealed together (Figure 8). One oligonucleotide contained a 3' disulfide attachment that would later be cleaved to allow for a sulfur bond to the gold nanograting. The other oligonucleotide contained a terminal Cy-3 attachment on the 3' end. When annealed, a now double strand of DNA deposited onto the gold nanograting would look like Figure 9. We chose

20 base pair strands so that the DNA would be positioned about 7nm away from the nanograting surface. Base pairs have a separation distance of 0.34nm, making 20 base pairs 6.8nm. For planar structures it was initially unclear if we should consider the system as a radiating dipole above a conducting surface or a resonant energy transfer akin to FRET. The differences between these two interpretations has, to our knowledge, not been tested in the literature. For example, the work by Ashwin et al. 2022, deposits fluorescent molecules atop a planar surface using a 50nm tall polymer with the fluorescent molecules uniformly distributed throughout the layer. Additional work by Zhao et al. 2012 coats gold nanorods in a 40nm thick silica layer with fluorescent molecules uniformly distributed throughout. Our previous work deposited fluorescent molecules within this 50nm regime. For these DNA experiments we chose 7nm as a starting point that was well within the this 40-50nm range.

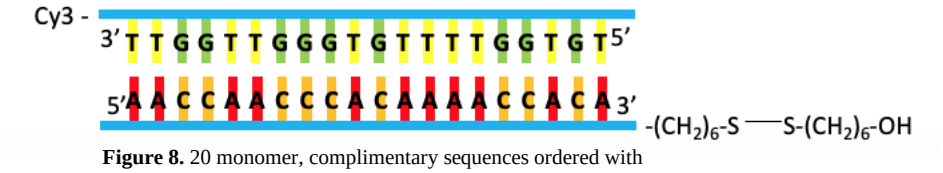

Figure 8. 20 monomer, complimentary sequences ordered with thiol and Cy3 attachments on the 3' ends

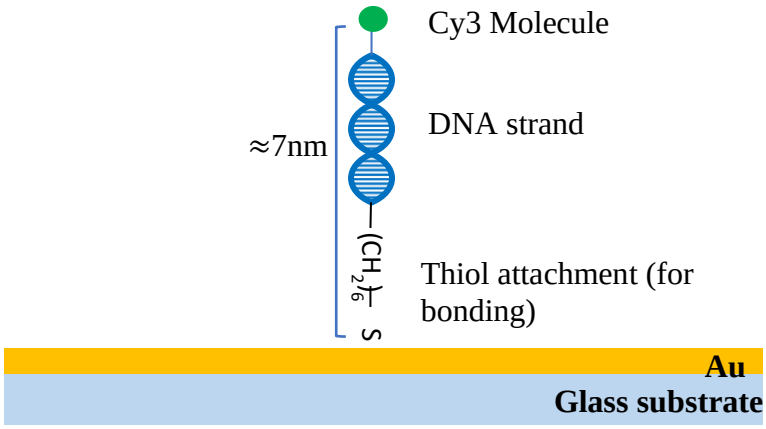

Figure 9. Concept of attaching Cy3 modified DNA to gold. Emphasis is placed on the thiol bond hence the scale. DNA strands are much larger than carbon chains.

ii. Annealing Procedure

The two oligonucleotides were annealed together prior to deposition. For these experiments a 10μM solution of annealed DNA was desired. Our procedure took components from Thermoscientific's 2009 procedure for annealing DNA. Stock solutions of thiol-modified DNA and Cy3-modified DNA were created in 100mM sodium phosphate, 150mM NaCl annealing buffer (pH 8.4). Prior to annealing, equal concentrations of thiol-modified solutions and Cy3 solution were made from the stock solutions and then combined in an amber microcentrifuge tube. The amber color helps prevent photobleaching. The strands were then annealed by placing the microcentrifuge tube in a 95℃-water bath for 5 minutes. The solution was then left at room temperature for one hour to cool.

After this cooling, the solution was stored in the fridge unless it was being used. Post annealing, 125μL of solution of dithiothreitol, abbreviated DTT ($C_4H_{10}O_2S_2$), was added to the solution and incubated at room temperature for 1 hour. DTT serves as a disulfide cleaving agent to break the disulfide bond on the thiol-modified, now double stranded, DNA, freeing up the sulfur atom still attached to the strand. This sulfur atom was what bonded to the gold during the deposition step. The solution was then purified using a NAP-10 column such that 10μM of annealed, cleaved DNA solution was eluted into a 100mM sodium phosphate buffer (pH 6.0) for more stable storage and were ready to use. The DTT cleaving process was adapted from Sigma-Aldrich and Hurst et al., 2006.

iii. Deposition onto Gold

The DNA is attached to gold via the free sulfur atom on the end of the helix chain post-cleaving. This procedure draws inspiration from the work of Steel et al., 1998, and Herne et al.,

1997. Thin gold films were produced a using template stripping method. Silicon wafers were sputter coated with gold then adhered, gold side down, to clean glass using a two-part epoxy. After being left overnight, the silicon wafer was peel off, leaving a thin gold film behind on the glass. A drop of DNA solution is then deposited onto a thin gold film sample.

During this initial deposition, the DNA sparsely covers the gold sample. The nitrogen in the DNA helix backbone is mildly attracted to gold. Consequently, the DNA may lean or lay sideways along the surface. To alleviate this problem, a spacer molecule is added in at a concentration of one thousand times that of the DNA to displace any nitrogen bonds and fill in the gaps between DNA, as illustrated in Figure 10. For all DNA strands, 6-mercapto-1-hexanol, abbreviated MCH ($C_6H_{14}OS$), was used as a spacer molecule. MCH was chosen because it has the same length carbon chain as the chain attached to the DNA strands.

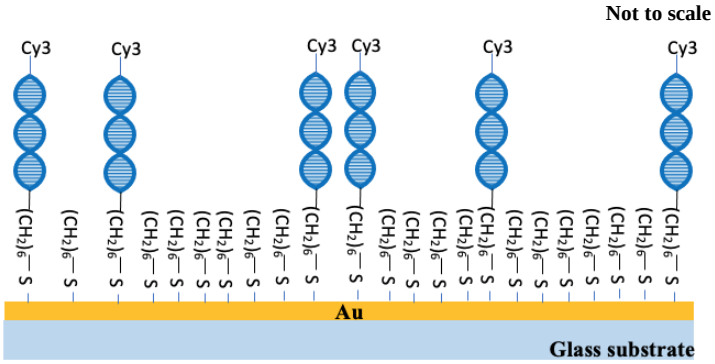

Figure 10. MCH spacer molecule fills in the gaps between DNA and forces the DNA to stand straight up. Emphasis in this diagram is on the chemical bonding. DNA strands are much large than the carbon chain.

Different combinations of DNA and MCH concentrations were tested for three parameters: highest density, closest average distance, and highest number of counts when the Cy3 molecule was excited by the laser. To carry this process out, the DNA solutions were diluted to test concentrations of 1μM, 3μM, 5μM, 7μM, and one was kept at 10μM. To test the parameters, the DNA was deposited onto thin gold films rather than the more expensive, time-

consuming gold nanogratings. A 100µL drop of each concentration was then deposited for one hour onto a thin gold film sample. The samples were monitored continuously for any signs of evaporation. If evaporation occurred, the sample was promptly rehydrated with another 100µL drop of the respective DNA solution. After 1 hour, the samples were rinsed three times with 18.2 MΩ MiliQ water.

Following the deposition of DNA and MiliQ water rinse, a 100µL drop of MCH was immediately deposited onto the sample. Again, the sample was left to sit for 1 hour with rehydration using the MCH solution if necessary. After 1 hour, the sample was again rinsed three times with 18.2 MΩ MiliQ water.

vi. Deposition onto Glass

To determine whether the surface plasmons on the air side of the gold nanograting would enhance the fluorescence, DNA was deposited onto a glass slide with no gold nanograting for reference. The sulfur group will not readily bond to glass, requiring that the glass be silanized prior to DNA deposition (Figure 11). The silane was (3-mercaptopropyl)trimethoxysilane, abbreviated MPTS ($HS(CH_2)_3Si(OCH_3)_3$). MPTS, when deposited onto a clean glass slide,

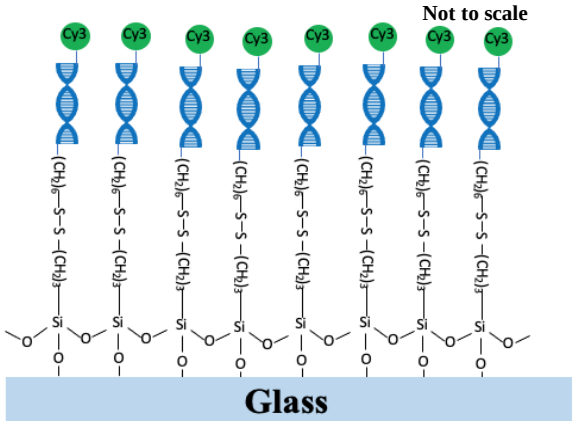

Figure 11. Illustration of DNA bonding to silanized glass. The sulfur group of the thiol attachment on the DNA binds to the free sulfur group on the silane compound.

followed by a DTT cleaving step, allows for the free sulfur on the DNA strand to bond to a free sulfur on the silane. The procedure for silanization and deposition of DNA was adapted from Rogers et al., 1998.

Glass slides were cleaned with an initial sonication in 3M potassium hydroxide (KOH) solution for 30 minutes. The slides were then rinsed with water 5 times. Following the rinse, the slides were sonicated in 200 proof ethanol for 30 minutes, rinsed with water 5 times again, and then sonicated in water for 30 minutes. All water used was 18.2 MΩ MiliQ water. The slides were dried with nitrogen gas then plasma cleaned for 12 minutes on medium.

For the silanization, clean glass slides were immersed in 5% MPTS, 95% ethanol overnight. The following day, the slides were removed from solution and immediately rinsed with ethanol and dried with nitrogen gas. The slides were transferred to a N_2 gas chamber and left to cure overnight. Upon curing, the slides were submerged in 10mM DTT solution for 30 minutes at room temperature. MPTS has a disulfide bond that, when broken, allows for easier bonding of the DNA sulfur chain to the silane.

Different concentrations of Cy-3 modified DNA solution were deposited in a 100uL drop onto the silanized glass to determine which concentration resulted in the closest density to the 5μM DNA deposition onto the gold nanograting. The sample was kept in a sealed container overnight to prevent evaporation. Because the DNA backbone is not attracted to any part of the silane or glass, no spacer molecule was required for the background slide.

iv. Characterization

To determine both the density of DNA deposited onto the gold nanograting as well as the average spacing between strands, epifluorescence scans were taken of each concentration

combination of DNA and MCH. Epifluorescence works by shining light of a specific wavelength to cause fluorescence from the molecule and generate an image. Figure 12, for example, shows the epifluorescence image for 5μM DNA, 5mM MCH deposited onto a thin gold film. Since a single Cy3 molecule is attached to each double stranded DNA, then each of the small, white spots in Figure 12 presumably indicates the presence of a single Cy3 molecule atop an individual DNA strand. The larger bright spots are likely clumps of DNA.

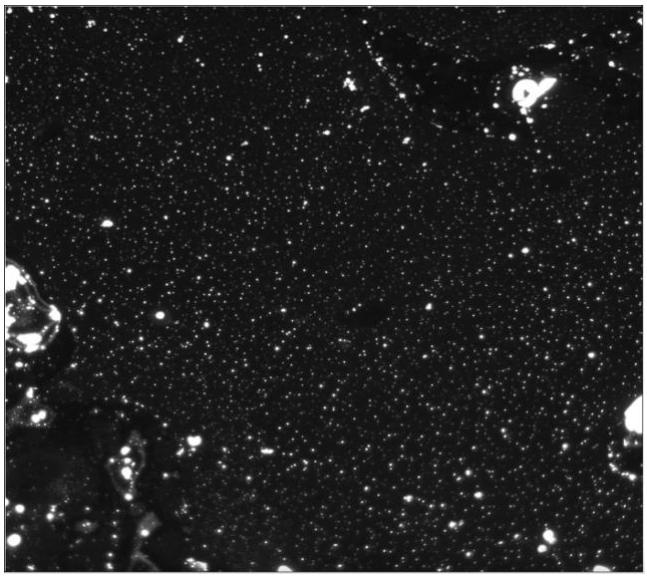

Figure 12. Epifluorescence scan of 5μM DNA, 5mM MCH deposited onto thin gold film. The small white dots are presumably individual donor molecules on single strands of DNA.

Epifluorescence images were first loaded into ImageJ, an image analysis software where each pixel corresponds to a brightness value. A code was written to run through the "Find Maxima" function through each image. Find Maxima requires a given prominence threshold. For a dark background image, only values above this prominence threshold will be flagged. The prominence is decided by the observer. For this dataset, the prominence was adjusted until nearly every point was flagged. Figure 13 depicts this maxima flagging. ImageJ allows for these maxima to be exported as pixel coordinates in a csv file. The csv files were then loaded into MATLAB where the title rows and columns were stripped, leaving only x and y coordinates.

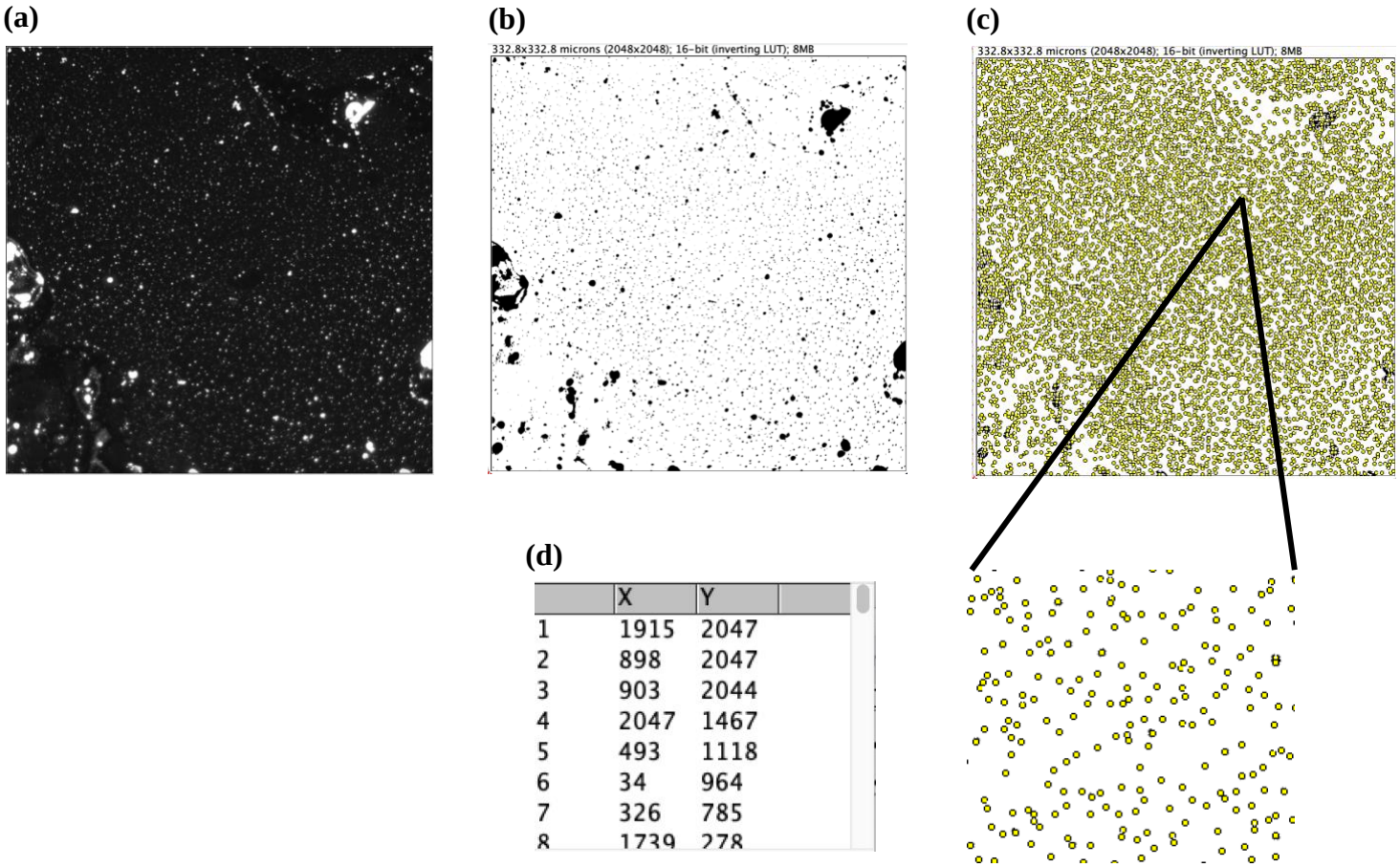

Figure 13. ImageJ Analysis process. (a) The same as Figure 12. (b) For ease on the eyes, the image is first inverted to black on white. The ImageJ macros does not actually need to do this to get the same maxima as if it were black and white. (c) Flagged maxima at 200 prominence with a zoomed in image to show that majority of the maxima in each space are indeed flagged with a single point. (d) these maxima are then exported into a table of positions corresponding to pixel coordinates.

A custom MATLAB code was written to calculate the density and nearest neighbor (NN) between DNA strands. The density is given by

$$D=N/A \qquad (3)$$

where D is the density, N is the number of maxima, and A is the area. The area was found by picking out the maximum and minimum of both the x and y coordinates. The minimum x was subtracted from the maximum x, and the same process was repeated for the y coordinate. The resulting values were multiplied together.

To determine the average NN distance, the code created a zero matrix to house calculated NN distances between individual points. A for loop then operates on a every row in the position matrix. It begins by removing the point being observed from the maxima position matrix. This is to prevent the point from being selected as its own NN and thus falsely giving a NN distance of zero. The MATLAB function knnsearch was then operated on the data to pick out the NN x and y position. The NN distance was then calculated using the distance formula

$$NN_{observed}=\sqrt{(x-x_{NN})^2+(y-y_{NN})^2} \qquad (4)$$

This distance is then inputted into the zero matrix prior to the loop repeating. When the loop concludes a list of all NN distances is outputted. Duplicate NN distances are allowed. The NN distance list is converted from pixels to microns and averaged to give a final observed distance.

v. Results

Table 1 contains the density, the observed average distances, the standard deviation, and the variance for each tested combination of DNA and MCH concentrations.

Table 1. Spatial values for DNA and MCH concentration combinations

DNA Concentration (μM)	MCH Concentration (mM)	Density (molec/(μm)^2)	Observed Avg. Dist. (μm)	Std. Dev.	Variance
1	0.2	0.0009	15.5	10.3	105.2
1	0.5	0.0005	21.5	19.6	385.8
1*	1	0.0002	16.3	-	-
3*	1	0.002	11.7	-	-
5	1	0.007	5.33	3.82	14.56
7	1	0.005	7.02	4.63	21.43
10	1	0.008	5.13	3.84	14.77
3	3	0.006	5.60	4.19	17.52
5	5	0.08	2.08	0.803	0.6441
10*	10	0.001	10.6	-	-

***** Denotes a set of data that required the values to be averaged from multiple images due to some images being blurry in certain portions. Thus a Std. Dev. and variance would be far too inaccurate to include in this table.

Images of each concentration deposited onto thin gold films are provided in Appendix 1. As seen by the table, the 5µM DNA and 5mM MCH had the most desirable parameters. The density of this concentration combination was the highest, and the expected and observed average distances were the lowest, meaning the DNA strands would be closer together for FRET to occur if we were to replace some of the donors with acceptors. Based on Figure 12, this concentration combination had less clumping than other concentrations shown in Appendix 1. 5µM DNA and 5mM MCH became the combination used in experiments going forward on gold nanogratings.

The same deposition process was repeated on a gold nanograting. Unlike thin gold films, the nanogratings have nanowires of gold with glass in between. The DNA, given its thiol bonding group will only bond to the gold regions, as illustrated in Figure 14. Again, for the deposition onto the gold nanograting, only the donor was deposited to verify attachment before adding an acceptor.

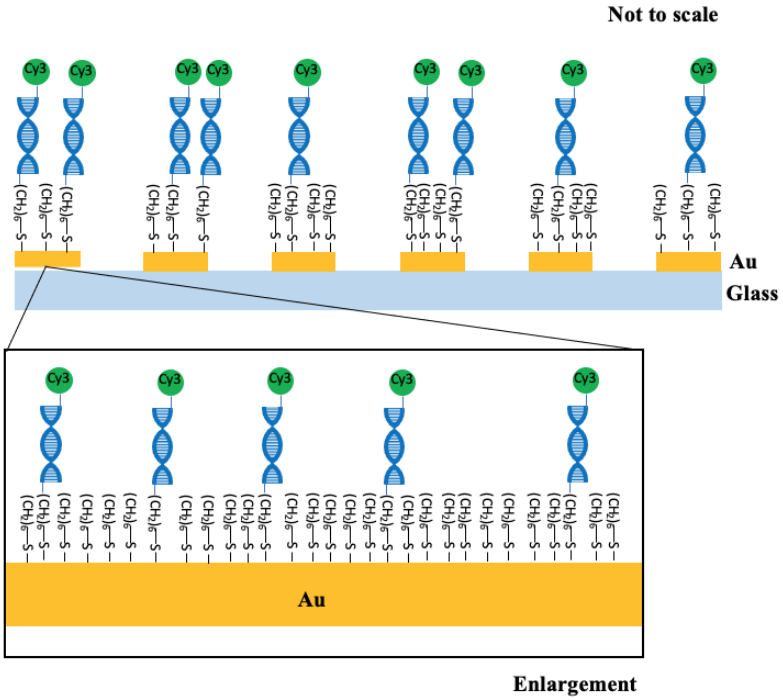

Figure 14. Illustration of DNA deposition onto a gold nanograting. An enlargement is included to show more accurate scale. Emphasis is placed on the bonding; DNA is much larger than a carbon chain.

The result of 5μM DNA and 5mM MCH deposition onto a gold nanograting with a height of 50nm and period of 500nm is shown in Figure 15. Small grating lines can be seen as white lines where the DNA has attached to the gold nanowire. The more obvious, macro lines are indicative of a super pattern the likely came about during the fabrication process. This super pattern had no noticeable effect on the ImageJ analysis of the image. The ImageJ and MATLAB codes were run on this image, and the data is provided in Table 2.

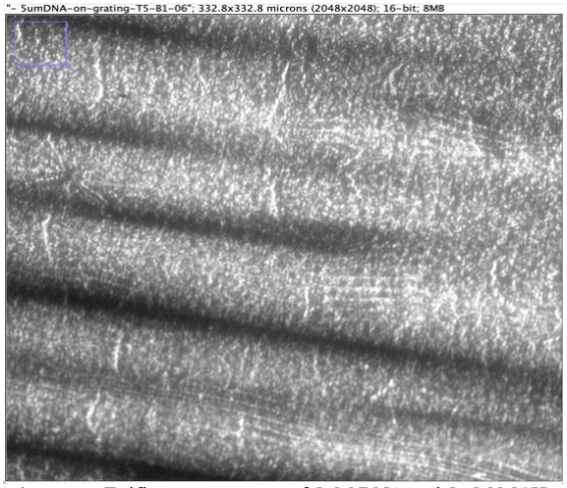

Figure 15. Epifluorescence scan of 5μM DNA and 5mM MCH deposited onto a gold nanograting.

Table 2. Spatial values of DNA on nanograting

Density	0.0633 molec/μm^2
Observed Average Distance	2.4μm
Std. Dev.	0.9μm

A glaring problem appears in the data for both thin gold films and gold nanograting regarding using this DNA structure for FRET analysis. In both the thin gold films and nanogratings, the separation between one DNA strand and its neighbor come out to be on the micron scale. The Förster radius is on the 1-10nm scale, requiring the DNA to deposit much closer. Pairing that with the reality that a DNA strand containing an acceptor molecule may not necessarily deposit as a nearest neighbor to a donor means that we cannot rely on the donor and acceptor being on separate DNA strands. A possible solution to this issue is presented in Section V.

V. Fluorescence Measurements

Before looking for FRET enhancement, we first verify that we get general fluorescence enhancement of our Cy3 donor by a surface plasmon on a nanograting. To do this we used a home-built apparatus that could change the angle of an incident green laser on the sample relative to the surface normal and the detector angle around the sample. The apparatus is illustrated in Figure 16. The sample is first placed in a holder that can rotate. A 532nm diode laser (the wavelength necessary to excite the Cy3 donor molecule) was shown on the sample relative to the surface normal. A fiber optic detector, also adjustable in angle relative to the surface normal, was used to collect fluorescence and fed into a CCD array from Ocean Optics (QEPro). We then initially rotated the sample such that the laser was incident at a 40° angle. 40° was chosen because according to the dispersion relationships we get from transmission (i.e., Figures 8a and 8b), we expect no excitation of surface plasmons as that angle. The dispersion relationship in Figure 7 indicated that excitation from the surface plasmon should occur in the -5° to 5° range. Thus, the detector was rotated between -5° and 20° in 1° increments to ensure the excitation angle of the surface plasmon would be included. The detector is covered with a 550nm high pass filter to filter out the excitation light. The same process was completed for the

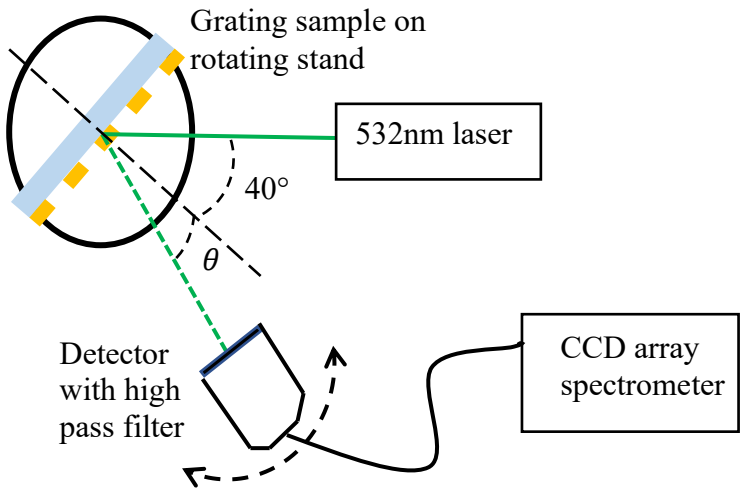

Figure 16. Custom apparatus for fluorescence measurements. The sample is rotated 40° relative to the 532nm laser, and a detector is swiveled around at angles we expect to see surface plasmons.

background slide. A MATLAB code was implemented to divide the actual data by the background data to detect any enhancement.

i. Terminally attached fluorophores on DNA

We placed the nanograting coated in our initial DNA structure (sample from Figure 15), with the donor terminally attached to the strand, inside the sample holder and took fluorescence measurements. We then followed up with a background slide containing 10μM DNA. Our goal was to see if we detected any enhancement of the fluorescence of the donor due to the surface plasmons. After running the MATLAB code with the obtained spectroscopic data, we expect to see a characteristic x-like shape depicted in Figure 17. Figure 17 shows the fluorescence enhancement of a donor molecule, Atto-532, in polyvinyl alcohol solution spin coated onto a gold nanograting. Additionally, if we were to plot the spectra at a given detector angle, we expect to see an enhancement at the corresponding surface plasmon wavelength according to Equation 2.

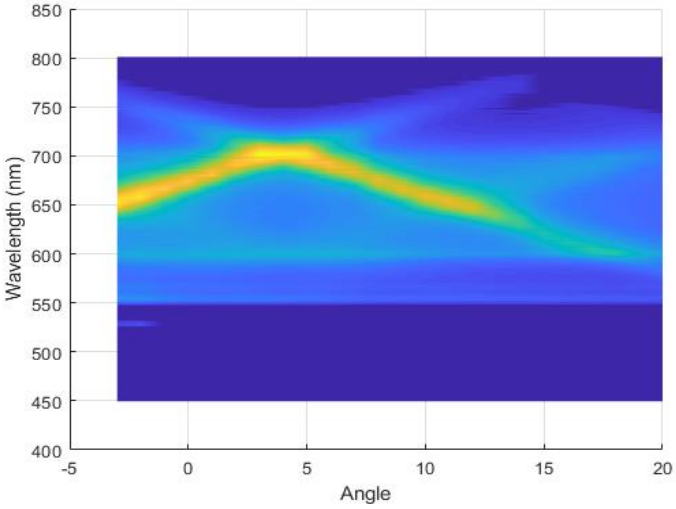

Figure 17. Fluorescence enhancement of Atto-532 donor molecule in polyvinyl alcohol solution. The x-like shape is similar to what expect to see in Cy3 enhancement

In Figure 17, the enhancement is slightly redshifted from the expected 500nm because the thin coating of PVA slightly raises the index of refraction. We do not expect this with the DNA solution. However, when we run the MATLAB code on the Cy3 terminally attached to DNA on the nanograting, we get the results depicted in Figure 18. Figure 18a shows the spectral data for the DNA coated nanograting, and Figure 18b shows the nanograting emission data divided by the background emission data.

(a) **(b)**

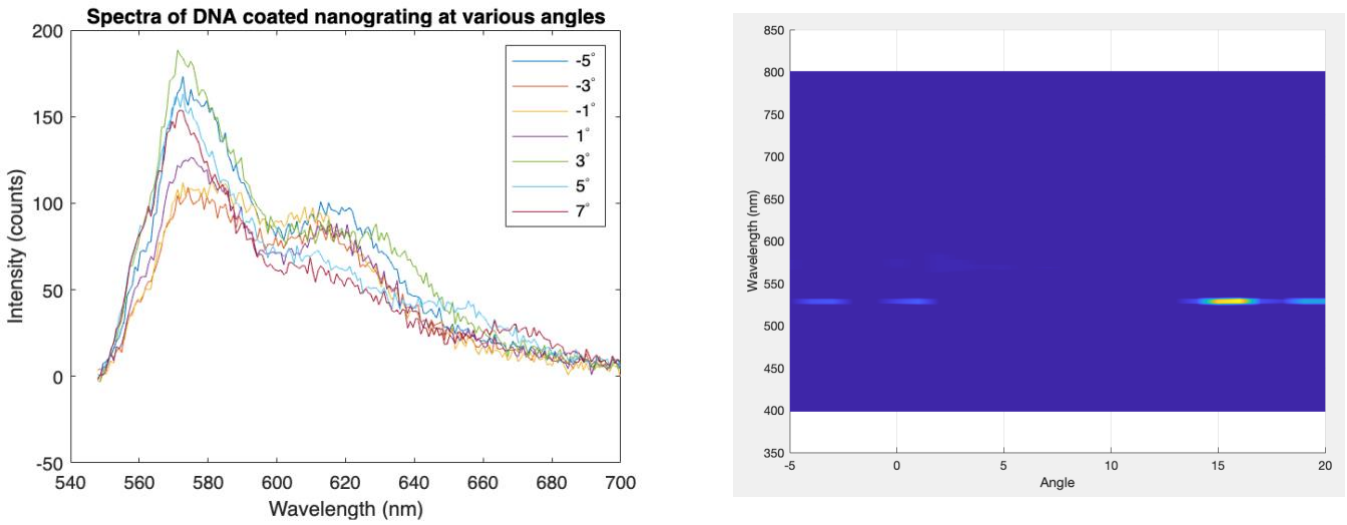

Figure 18. Results for Cy3 fluorescence measurements. (a) Spectra of the nanograting at various angles. We expect to see a shoulder on each of these curves representing the wavelength that the surface plasmon is enhanced at given the angle. (b) result of dividing the nanograting data by the background data with no indication of fluorescent enhancement.

From Figure 18a, we see that the shoulder (rightmost peak of the spectra) shifts slightly as we change the angle. This shift is indicative of surface plasmon enhancement at specific wavelengths that excite the surface plasmons, as we expect given Equation 2. Figure 18b, however, shows that there is no enhancement of fluorescence. Initially, the error seems to stem from the remarkably low numbers of counts at each wavelength in Figure 18a. However, further research into the properties of the Cy3 molecules suggest two potentially broader issues with the

chosen DNA structure: orientation of the Cy3 molecule on the terminal end and the distance of the molecule from the nanograting.

.

VI. Conclusions and Future Directions

We are currently investigating two potential sources of the lack of fluorescent enhancement: orientation of the dipole moment with respect to the surface and the distance between the fluorescent molecule and the surface. Fluorophores emit light via dipole radiation. Because of this dipole interaction, the orientation with respect to the nanograting is important. The dipole moment of a Cy3 molecule is displayed in Figure 19a. The Cy3 molecule bonds to the DNA backbone via phosphorylation on one end of the Cy3 molecule (phosphorus group involved is depicted in Figure 19b). However, the other end of the Cy3 molecule feels a Van der Waals attraction to the opposite backbone of the helix when attached on a terminal end of DNA.

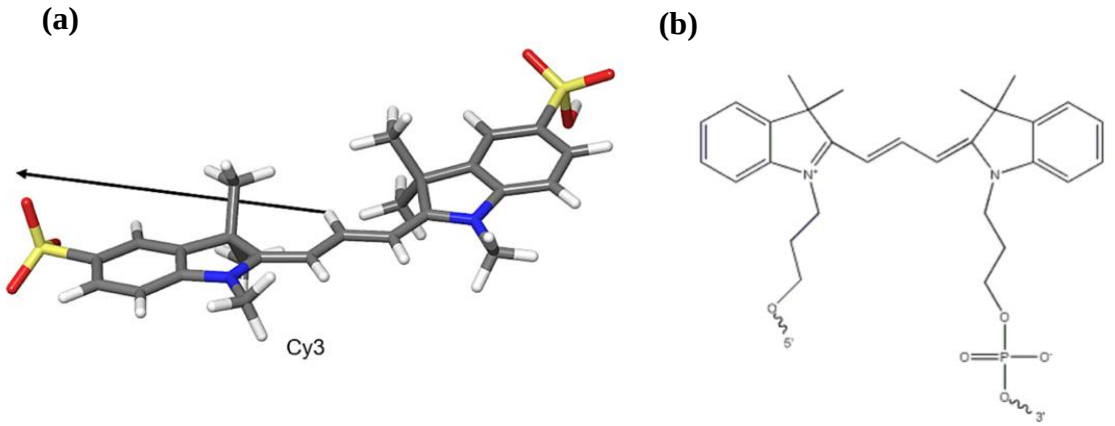

Figure 19. Diagrams of Cy3 molecule. (a) The dipole moment of the Cy3 molecule. (b) The structure of the Cy3 molecule. It attaches to the DNA via phosphorylation. Figure 19a provided courtesy of Dr. Christina Cooley, Trinity University Chemistry Department.

Thus, the Cy3 molecules lies nearly flat across the end of the helix (Lilley et al., 2011), forcing the dipole moment to lie nearly parallel with the nanograting rather than pointing upwards as we initially suspected. Figure 20 illustrates this concept.

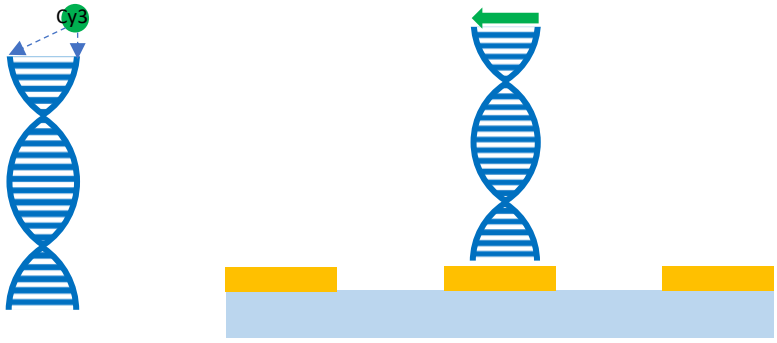

Figure 20. The strand on the left shows the two areas that the Cy3 molecule is attracted to (it binds to the backbone directly and is mildly attracted to the other end of the helix. The strand on the right shows Cy3's likely dipole orientation relative to the grating.

To address the second potential issue, we are investigating the fluorescent enhancement as a function of distance to the surface. We suspect our initial guess of 6.8nm may not have been optimized for enhancement. The lack of enhancement, as shown in Figure 18b, seems to indicate that treating surface plasmon enhanced fluorescence as RET, rather than a dipole radiating above a conducting surface, is appropriate.

Fluorophores attached internally along DNA backbone

To remedy the possible misorientation of the Cy3 dipole moment relative to the nanograting, we ordered new strands of DNA that had the Cy3 molecule internally attached to the DNA backbone. This modification also allows for the acceptor to eventually be positioned some known distance along the backbone as well, circumventing the nearest neighbor issue that arose during the deposition analysis where the DNA were separated on a micron scale. By placing both donor and eventually acceptor on the backbone, they are now separated on an angstrom scale that can be fine tuned and no longer depend on a neighboring DNA strand for FRET. Lastly, we sought to vary the distance of the donor to the nanograting and chose distances

of 10 base pairs (3.4nm), 20 base pairs (6.8nm, for a control group), and 30 base pairs (10.2nm) from the nanograting surface. In total, 4 new strands were ordered. One strand contained a thiol modification on the terminal end to attach to gold. The other three strands were complimentary to the thiol strand with a Cy3 donor molecule internally attached. The final annealed strands deposited onto the nanograting are illustrated in Figure 21.

The DNA was deposited onto the gold using the same method described in Section IV. Three background slides were manufactured for each type of annealed DNA strands. Fluorescence measurements were taken using the same appartus and methods described earlier in this section.

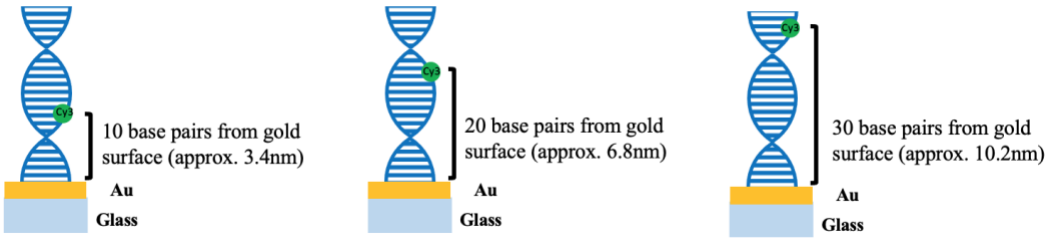

Figure 21. Illustration of new ordered and annealed DNA strands. Distances, both in base pairs and nanometers, of the Cy3 molecule from the nanograting are varied. All strands contain an internal Cy3 modification rather than a terminal attachment.

The spectra of the nanograting at various angles and the fluorescence enhancement graph are plotted in Figure 22 for the strand with the donor internally added 20 base pairs away from the nanograting. The strands with the donor 10 base pairs and 30 base pairs away should not enough attachment for a fluorescence measurement.

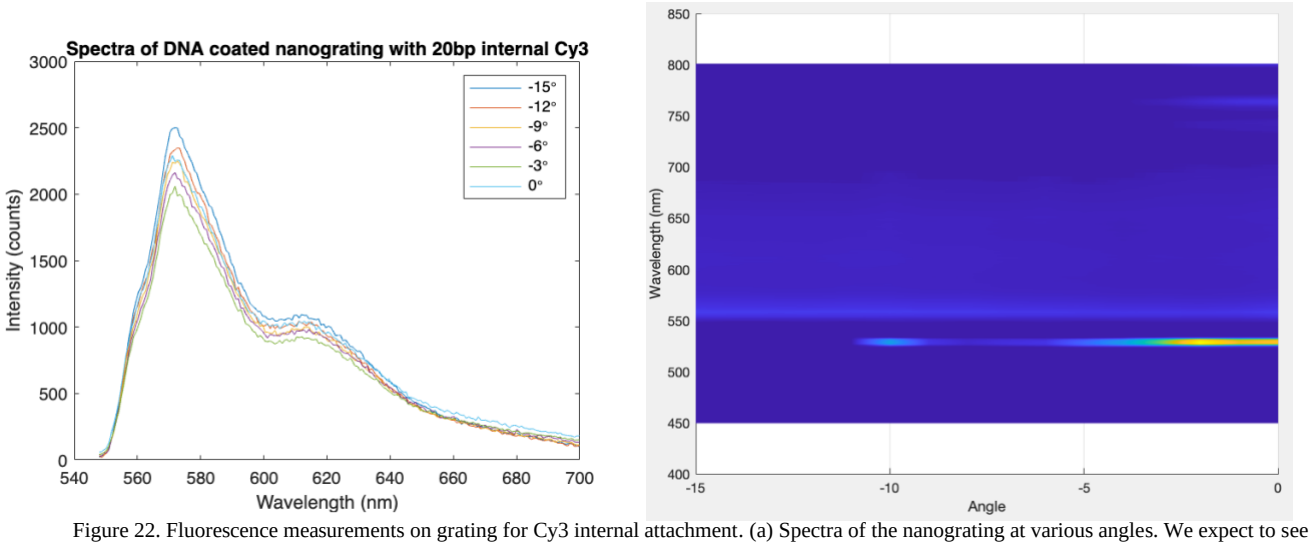

Figure 22. Fluorescence measurements on grating for Cy3 internal attachment. (a) Spectra of the nanograting at various angles. We expect to see a shoulder on each of these curves representing the wavelength that the surface plasmon is enhanced at given the angle. (b) result of dividing the nanograting data by the background data with no indication of fluorescent enhancement.

Again, we see no fluorescence enhancement in Figure 22b. Unlike Figure 18a, we also do not see any kind of shoulder shift on the spectra indicating a surface plasmon excitation. The only parameter that changed between the sample in Figure 18 and the one in Figure 22 was the position of the Cy3 being terminal and internal, respectively. From Figures 20 and 21, we have reason to believe that a terminal Cy3 and an internal Cy3 molecule will have different dipole orientations. Because neither sample showed fluorescence enhancement, this initial data suggests that dipole orientation was not the cause.

Future experiments will need to repeat the deposition and fluorescence measurements of the internally modified 20bp DNA sample to determine if these results are consistent. Additionally, more trials of the 10bp and 30bp internal modifications will need to be conducted

to determine if a closer or further distance of the Cy3 molecule from the nanograting will enable fluorescence enhancement.

Once fluorescence enhancement is detected, the Cy5 acceptor molecule will be added to the DNA strand at a chosen distance away from the donor to undergo FRET. Initial experiments will position the acceptor further away from the nanograting, but eventually the donor and acceptor will be switched such that the acceptor is closer to the nanograting. We will then analyze the effect that donor and acceptor distance have relative to each other and the surface plasmon and if such modifications would affect FRET enhancement.

VII. Works Cited

Herne, Tonya M.; Tarlov, Michael J. "Characterization of DNA Probes Immobilized on Gold Surfaces" *Journal of the American Chemical Society*, vol. 119, no. 38, 24 September 1997, pp. 8916-8920.

Hure, Robert; Simoneau, Samuel; Chandler, Bert D.; Steele, Jennifer M. **"**Two-Color Metal-Enhanced Fluorescence Using Gold Slotted Nanogratings." *Plasmonics*, vol. 12, 21 November 2016, pp. 1621–1626.

Hurst, Sarah J.; Lytton-Jean, Abigail K. R.; Mirkin, Chad A. "Maximizing DNA loading on a range of gold nanoparticle sizes." *Analytical Chemistry*, vol. 78, no. 24, 01 December 2006, pp. 8313-8318.

Lackowicz, Joseph R. *Principles of Fluorescence Spectroscopy*. Springer. 2006.

Lilley, David M.J.; Wilson, Timothy J.; Iqbal, Asif; Schorr, Stephanie; Ouellet, Jonathan. "Orientation of Cyanine Fluorophores Terminally Attached to DNA via Long, Flexible Tethers. *Biophys J.*, vol. 101, no. 5, 7 September 2011, pp. 1148-1154.

Raether, Heinz. *Surface Plasmons on Smooth and Rough Surfaces and on Gratings*. Springer-Verlag. 1998.

Rogers, Yu-Hui et al. "Immobilization of Oligonucleotides onto a Glass Support via disulfide Bonds: A Method for Preparation of DNA Microarrays." Analytical Biochemistry, vol. 266, 8 May 1998, pp. 23-30.

Sigma-Aldrich, "Protocol for Thiol-Modified Oligonucleotide DDT Reduction." *Millipore Sigma*, https://www.sigmaaldrich.com/US/en/technical-documents/protocol/materials-science-and-engineering/drug-delivery/oligo-reduction

Steel, Adam B; Herne, Tonya M.; Tarlov, Michael J. “Electrochemical Quantitation of DNA Immobilized on Gold.” *Analytical Chemistry*, vol. 70, no. 22, 15 November 1998, pp. 4670-4677.

Steele, Jennifer M.; Ramnarace, Chae; Farner, Will. “Controlling FRET Enhancement Using Plasmon Modes on Gold.” *J. Phys. Chem.*, vol. 121, no. 40, 18 September 2017**,** pp. 22353–22360**.**

Steele, Jennifer M.; Gagnidze, Iuri; Wiele, Stephanie M. “Efficient Extraction of Fluorescence Emission Utilizing Multiple Surface Plasmon Modes from Gold Wire Gratings.” *Plasmonics*, vol. 5, 17 June 2010, pp. 319-324**.**

Thermoscientific. “Anneal complimentary pairs of oligonucleotides.” *Thermo Fisher Scientific Inc.* 2009.

Appendix 1: Epifluorescence Images for various DNA/MCH combinations

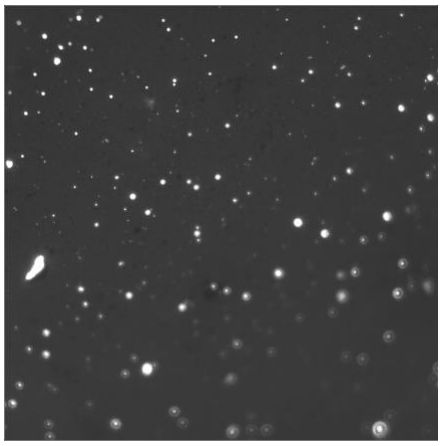

1uM DNA, 1mM MCH

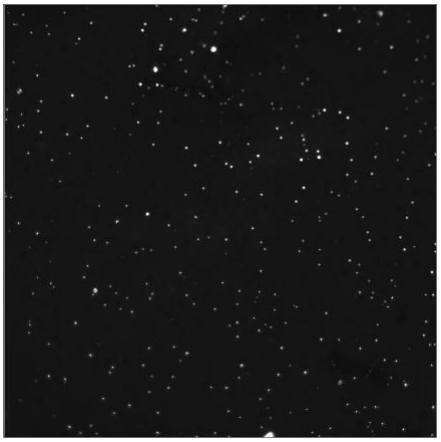

3uM DNA, 3mM MCH

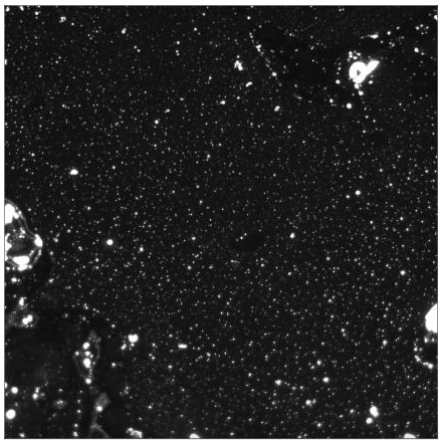

5uM DNA, 5mM MCH

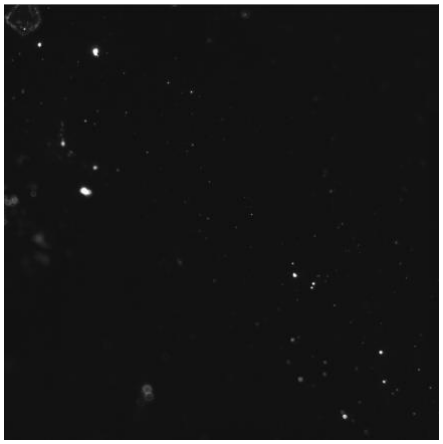

10uM DNA, 10mM MCH

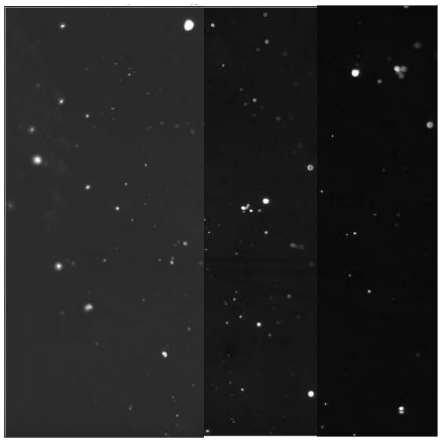

3uM DNA, 1mM MCH

5uM DNA, 1mM MCH

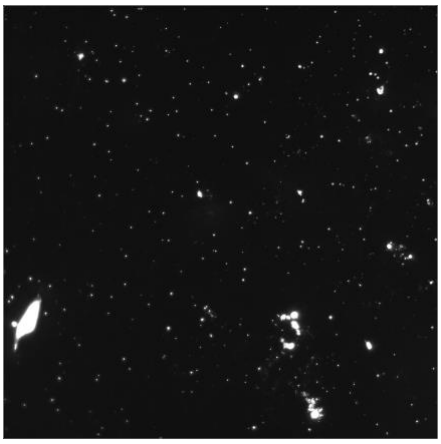

10uM DNA, 1mM MCH

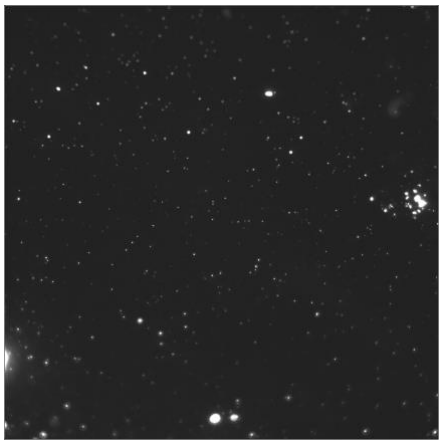

7uM DNA, 1mM MCH

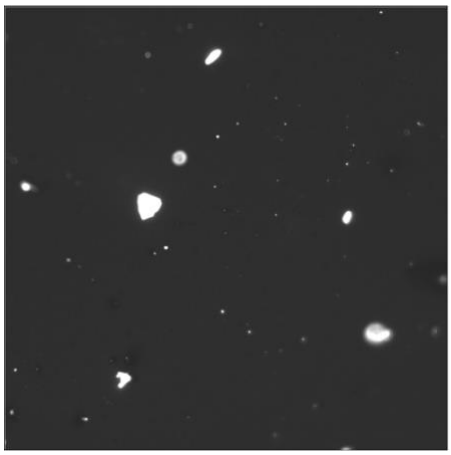

1uM DNA, 0.5mM MCH

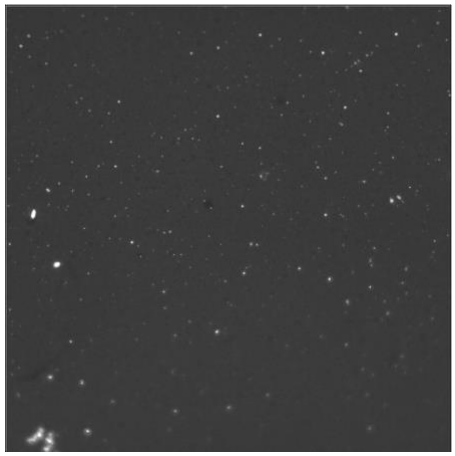

1uM DNA, 0.2mM MCH

Appendix 2: ImageJ and MATLAB NN Codes

```
setBatchMode(true);
  imgArray = newArray(nImages);
  for (i=0; i<nImages; i++) {
    selectImage(i+1);
    imgArray[i] = getImageID();
}
//now we have a list of all open images, we can work on it:
for (i=0; i< imgArray.length; i++) {
  selectImage(imgArray[i]);
  Name=getTitle();
  run("Find Maxima...", "prominence=200 output=List");
  saveAs("Results", "/Users/evan/Documents/"+Name+".csv");
}
```

```
%Note: remove any semicolons to see what the output is, but inside the loop,
%removing semicolons can dramatically slow down the process. For any
%troubleshooting, it is recommended you use the "TestImageJ_code" that only has five points rather than thousands.



% Importing Data and eliminating title rows and columns that come with the csv file.
MaximaPositions=readmatrix(filename); %readmatrix reads in a csv file. Iaso reads in text files, but csv is what ImageJ generates.
MaximaPositions(1,:)=[]; %[] removes the row/column from the matrix
MaximaPositions(:,1)=[]; %outputs a matrix of maxima positions in x and y coordinates



%Calculation of Density
N=length(MaximaPositions(:,1)); %number of maxima
A=(332.8)^2; %area in microns (read out at the top of ImageJ)
```

```
Density=(N/A) %per micron squared


%Theoretical calculation of average distance using Inverse Square Law.
%Note, the 0.5 term comes from a 1954 derivation that originates from a Poisson
%Distribution and it applicable to this kind of spread. See References 1 (section 3.1) and 2
(Appendix).
ExpAvgDist=0.5*(Density)^(-1/2)



i=length(MaximaPositions); %length of maxima positions matrix is how many maxima you have
ZeroArray=zeros([i 1]);
for n=1:i
    Y=MaximaPositions(n,:);
    MaximaPositions(n,:)=[];
    T=knnsearch(MaximaPositions,Y);
    NearestNeighbor=MaximaPositions(T,:);
%recreating the maxima matrix
    ReInsert=Y;
    if n==1
        MaximaPositions=[ReInsert;MaximaPositions(n:i-1,:)];
    elseif n==i
        MaximaPositions=[MaximaPositions(1:n-1,:);ReInsert];
    else
        MaximaPositions=[MaximaPositions(1:n-1,:);ReInsert;MaximaPositions(n:i-1,:)];
    end
%generating a matrix of distances
    Distance=sqrt((NearestNeighbor(1,1)-MaximaPositions(n,1)).^2+(NearestNeighbor(1,2)-
MaximaPositions(n,2)).^2);
    ZeroArray(n)=Distance;
end
```

```
ListOfDistances=ZeroArray;


U=length(unique(ListOfDistances));


%Conversion from pixels to microns
List=ListOfDistances.*0.1625;


%Observed Distance
AvgDistObs=(sum(List, 'all'))/length(MaximaPositions)
%Variance Calculation for observed diatance
ListSquared=List.^2; %Just squares the List matrix
AvgSquared=(sum(ListSquared, 'all'))/(length(MaximaPositions));
Variance=AvgSquared-AvgDistObs^2
StdDev=sqrt(Variance)
```